Beamforming Design for Active IRS-Aided MIMO Integrated Sensing and Communication Systems

Jin Li, Gui Zhou, *Member, IEEE*, Tantao Gong, and Nan Liu, *Member, IEEE*

***Abstract*—This letter investigates active intelligent reconfigurable surface (IRS)-aided MIMO integrated sensing and communication (ISAC) systems. Different from passive IRS, an active IRS with amplifiers is deployed to overcome the product attenuation caused by the reflection of the IRS. We aim to maximize IRS beampattern towards the direction of a point sensing target, while guaranteeing the quality of service (QoS) requirement of the communication user. The target is sensed by the reflected sensing link, and the user can receive communication signals from both the direct link and the reflected link. To solve the formulated problem with coupled variables, an alternating optimization algorithm is proposed. Approximations such as the majorization-minimization (MM) method is used to tackle the BS beamforming subproblem, while some matrix transformations, the semidefinite relaxation and the Gaussian randomization method is applied to solve the reflection coefficient subproblem. Numerical results demonstrate that active IRS can greatly improve the sensing performance compared to passive IRS.**

***Index Terms*—Integrated sensing and communication (ISAC), active intelligent reconfigurable surface (IRS), beamforming, majorization-minimization (MM), semidefinite relaxation (SDR).**

I. Introduction

INTEGRATED sensing and communication (ISAC) has been viewed as a promising technology to alleviate the crowdedness of the existing spectrum in the next generation wireless communication system. Additionally, compared to the conventional radar communication coexistence (RCC) system, ISAC system can bring better efficiency of energy and hardware with the unification of radar system and communication system.

The sensing task is often considered with the assistance of the direct link between the BS and the sensing targets. However, when the direct link is blocked by some obstacles such as buildings, it is challenging for the BS to perceive targets. To address this issue, intelligent reconfigurable surfaces (IRS) are used, which can create an additional reflected sensing link between the BS and the targets [1]. Recently, the authors of [1] maximized the minimum radar beampattern towards the sensing targets while ensuring the requirement of communication in the scenario of passive IRS-aided ISAC systems. It is shown that when the direct link between the BS and the target is blocked by some obstacles, passive IRS-aided sensing can simultaneously achieve good beampattern and guarantee the performance of the communication task. Nevertheless, multiplicative fading, which is caused by the product attenuation in the BS-IRS-target-IRS-BS sensing link and the BS-IRS-user communication link, can lead to negative effects on IRS-aided ISAC systems. Additionally, if the pathloss of the signal propagation environment is very large [2], the echo signal received by the BS and the received signal at the user can be very weak. In these cases, rather than using passive IRS, active IRS equipped with active reflective amplifiers can mitigate multiplicative fading [3]. With the aid of active IRS's amplification, the strength of the echo signal at the BS and the received signal at the user can be greatly improved. It has also been shown that the average secrecy rate can be greatly improved in active IRS-aided ISAC secrecy systems [4].

Against this background, this letter investigates active IRS-assisted MIMO ISAC systems, where a point target is perceived via the IRS-aided sensing link, i.e., BS-IRS-target-IRS-BS link, and a single-antenna user communication is accomplished by both direct and IRS reflected link. Both dual-functional radar-communication (DFRC) MIMO BS and active IRS, which is assumed to work as a colocated MIMO radar, are equipped with the uniform linear array (ULA). We aim to maximize the IRS beampattern gain towards the direction of the sensing target under communication rate constraint, active IRS and BS transmit power constraints, and IRS amplifiers' reflection gain constraints. The formulated optimization problem is highly coupled and nonconvex, so an alternating optimization (AO) algorithm is applied. Approximations such as the Majorization-Minimization (MM) method is used to solve the BS beamforming subproblem. Then, the reflection coefficients subproblem is solved using semidefinite relaxation (SDR) and Gaussian randomization methods, wherein some matrix transformations are used to tackle two quartic terms and the nonconvex objective function. Numerical results show that with the same total transmit power, our proposed ISAC beamforming scheme could achieve better beampattern with less reflecting elements compared to ISAC beamforming scheme based on the passive IRS.

II. System Model

As shown in Fig. 1, we consider an active IRS-aided MIMO system, wherein the DFRC BS is equipped with N_T transmit antennas and N_R receive antennas. It is assumed that the BS serves a single-antenna communication user and perceives a point target simultaneously. For the sensing task, we assume that the direct link between the sensing target and the BS is

Manuscript received 7 June 2023; accepted 4 July 2023. Date of publication 18 July 2023; date of current version 9 October 2023. This work was supported in part by the National Natural Science Foundation of China under Grant 62071115 and Grant 61971135, and in part by the Research Fund of National Mobile Communications Research Laboratory, Southeast University under Grant 2023A03. The associate editor coordinating the review of this article and approving it for publication was D. Mishra. *(Corresponding author: Nan Liu.)*

Jin Li, Tantao Gong, and Nan Liu are with the National Mobile Communications Research Laboratory, Southeast University, Nanjing 211189, China (e-mail: lijin@seu.edu.cn; gongtantao@seu.edu.cn; nanliu@seu.edu.cn).

Gui Zhou is with the Institute for Digital Communications, Friedrich-Alexander-University Erlangen-Nürnberg, 91054 Erlangen, Germany (e-mail: gui.zhou@fau.de).

Digital Object Identifier 10.1109/LWC.2023.3294537

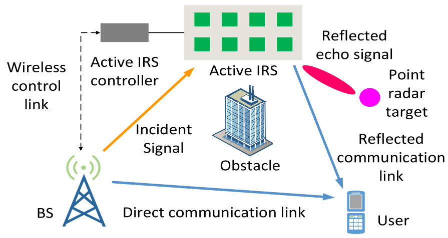

Fig. 1. An active IRS-aided integrated sensing and communication system.

blocked by an obstacle, and a reflected sensing link is created with the assistance of the IRS [1], i.e., BS-IRS-target-IRS-BS sensing link. However, the product attenuation caused by the multiple reflections is very severe in passive IRS-aided ISAC systems [2]. Thus, in order to mitigate the effect of attenuation, we deploy an active IRS which has the function of the phase shift, and additional amplifier for every reflecting element compared to the traditional passive IRS [3]. The active IRS has M reflecting elements and the reflection coefficient matrix is represented by $\mathbf{E} = \mathrm{diag}(e_1, e_2, \ldots, e_M) \in \mathbb{C}^{M\times M}$, where the amplification gain of the m-th reflecting element is limited to $0 < |e_m|^2 \leq p_{max}$ and p_{max} is the maximum amplification gain.

The transmit DFRC signal at the BS is given by $\mathbf{x} = \mathbf{w}s$, where vector $\mathbf{w} \in \mathbb{C}^{N_T\times 1}$ denotes the dual-functional beamforming, and $s \in \mathbb{C}^{1\times 1}$ is the data symbol, which follows the complex Gaussian distribution with zero mean and unit variance, i.e., $\mathbb{E}\{ss^*\} = 1$. Thus, the BS transmit power is given by $\mathbb{E}\{\|\mathbf{x}\|^2\} = \|\mathbf{w}\|_2^2$. The BS also designs the reflection coefficients matrix of the active IRS which can be sent back to the IRS controller via the wireless control link as shown in Fig. 1. Let's denote the channels[1] between the BS and the IRS, the IRS and the user, and the BS and the user as $\mathbf{H}_{\mathrm{BI}} \in \mathbb{C}^{M\times N_T}$, $\mathbf{h}_{\mathrm{IU}} \in \mathbb{C}^{M\times 1}$ and $\mathbf{h}_{\mathrm{BU}} \in \mathbb{C}^{N_T\times 1}$, respectively.

In terms of the communication function, the received signal at the user can be written as follows

$$y_c = \mathbf{h}_{\mathrm{BU}}^H\mathbf{x} + \mathbf{h}_{\mathrm{IU}}^H\mathbf{E}(\mathbf{H}_{\mathrm{BI}}\mathbf{x} + \mathbf{n}_I) + n_c, \tag{1}$$

where $\mathbf{n}_I \in \mathbb{C}^{M\times 1}$ and $n_c \in \mathbb{C}$ are the additive white Gaussian noise (AWGN) caused by the amplifier of the active IRS and received at the user, which follows the distributions $\mathbf{n}_I \sim \mathcal{CN}(\mathbf{0}, \sigma_I^2\mathbf{I}_M)$ and $n_c \sim \mathcal{CN}(0, \sigma_c^2)$ with noise power σ_I^2 and σ_c^2, respectively.

To evaluate the communication performance, transmission rate at the user is chosen as our design criterion which can be written as

$$R = \log_2\left(1 + \frac{|(\mathbf{h}_{\mathrm{BU}}^H + \mathbf{h}_{\mathrm{IU}}^H\mathbf{E}\mathbf{H}_{\mathrm{BI}})\mathbf{w}|^2}{\sigma_I^2\|\mathbf{h}_{\mathrm{IU}}^H\mathbf{E}\|^2 + \sigma_c^2}\right). \tag{2}$$

The amplified transmit reflected signal at the active IRS can be represented as

$$\mathbf{y}_1 = \mathbf{E}(\mathbf{H}_{\mathrm{BI}}\mathbf{x} + \mathbf{n}_I), \tag{3}$$

which is used to probe the sensing target.

[1]The individual channels, i.e., $\mathbf{H}_{\mathrm{BI}}$, $\mathbf{h}_{\mathrm{IU}}$, and $\mathbf{h}_{\mathrm{BU}}$, can be estimated with the aid of two single-antenna anchors as in [5]. It is assumed that the channel state information (CSI) is perfectly known at the BS.

Similar to (3), the amplified receive reflected signal at the active IRS can be represented as [6]

$$\mathbf{y}_2 = \mathbf{E}^H(\mathbf{G}\mathbf{E}(\mathbf{H}_{\mathrm{BI}}\mathbf{x} + \mathbf{n}_I) + \mathbf{n}_p), \tag{4}$$

where $\mathbf{n}_p$ is also the AWGN caused by the amplifier and independent of s and $\mathbf{n}_I$ and follows the complex Gaussian distribution $\mathbf{n}_p \sim \mathcal{CN}(\mathbf{0}, \sigma_p^2\mathbf{I}_M)$ with noise power σ_p^2.

We can assume that the distance between the active IRS and the sensing target is far, so that the target can be regarded as a point target [7]. Moreover, supposing that the active IRS works as a monostatic colocated MIMO radar [7], i.e., the angle of arrival (AOA) is equal to the angle of departure (AOD). Based on this, the target response matrix $\mathbf{G} \in \mathbb{C}^{M\times M}$ between active IRS and the sensing target can be modeled as [8]

$$\mathbf{G} = \beta\mathbf{a}(\theta)\mathbf{a}^H(\theta), \tag{5}$$

where θ is the AOA/AOD of the target relative to the active IRS, β is the complex amplitude which contains round-trip path-loss and the radar cross section of the target [4], [8], and $\mathbf{a}(\theta) = [1, e^{i\frac{2\pi d}{\lambda}\sin\theta}, \ldots, e^{i\frac{2\pi(M-1)d}{\lambda}\sin\theta}]$ is the steering vector of the active IRS. Here, λ is the wavelength, and $d = \frac{\lambda}{2}$ denotes the reflecting element spacing.

As for the design criterion of sensing performance, the transmit beampattern[2] at the active IRS towards the given direction θ is considered and given by [9], [10]

$$\begin{aligned}\mathbb{E}\{\mathbf{a}^H(\theta)\mathbf{y}_1\mathbf{y}_1^H\mathbf{a}(\theta)\} &= \mathbf{a}^H(\theta)\mathbf{E}\mathbf{H}_{\mathrm{BI}}\mathbf{w}\mathbf{w}^H\mathbf{H}_{\mathrm{BI}}^H\mathbf{E}^H\mathbf{a}(\theta)\\ &\quad + \sigma_I^2\mathbf{a}^H(\theta)\mathbf{E}\mathbf{E}^H\mathbf{a}(\theta).\end{aligned} \tag{6}$$

Here, we only focus on maximizing the transmit beampattern in the direction of desired point target. The initial target's location can be obtained by the generalized likelihood ratio test (GLRT) or Capon spectrum [9].

Then, the amplified power of the signal at the IRS is represented as

$$\begin{aligned}&\mathbb{E}\{\|\mathbf{E}(\mathbf{H}_{\mathrm{BI}}\mathbf{x} + \mathbf{n}_I)\|^2 + \|\mathbf{E}^H(\mathbf{G}\mathbf{E}(\mathbf{H}_{\mathrm{BI}}\mathbf{x} + \mathbf{n}_I) + \mathbf{n}_p)\|^2\}\\ &= \|\mathbf{E}\mathbf{H}_{\mathrm{BI}}\mathbf{w}\|_2^2 + \sigma_I^2\|\mathbf{E}\|_F^2 + \|\mathbf{E}^H\mathbf{G}\mathbf{E}\mathbf{H}_{\mathrm{BI}}\mathbf{w}\|_2^2 + \sigma_p^2\|\mathbf{E}\|_F^2\\ &\quad + \sigma_I^2\|\mathbf{E}^H\mathbf{G}\mathbf{E}\|_F^2.\end{aligned} \tag{7}$$

where the first two terms are amplified power of signals transmitted from the BS to the IRS, and the last three terms are amplified power of signals scattered by the radar target.

A. Problem Formulation

We jointly design the BS beamforming vector $\mathbf{w}$ and IRS reflection coefficient matrix $\mathbf{E}$ to maximize the transmit beampattern at the active IRS under the communication rate constraint. Then, the optimization problem can be formulated as follows

$$\max_{\mathbf{w},\mathbf{E}} \ \mathbf{a}^H(\theta)\mathbf{E}\mathbf{H}_{\mathrm{BI}}\mathbf{w}\mathbf{w}^H\mathbf{H}_{\mathrm{BI}}^H\mathbf{E}^H\mathbf{a}(\theta) + \sigma_I^2\mathbf{a}^H(\theta)\mathbf{E}\mathbf{E}^H\mathbf{a}(\theta) \tag{8a}$$

$$\text{s.t.} \ \|\mathbf{w}\|_2^2 \leq P_0, \tag{8b}$$

$$\|\mathbf{E}\mathbf{H}_{\mathrm{BI}}\mathbf{w}\|_2^2 + (\sigma_I^2 + \sigma_p^2)\|\mathbf{E}\|_F^2 + \|\mathbf{E}^H\mathbf{G}\mathbf{E}\mathbf{H}_{\mathrm{BI}}\mathbf{w}\|_2^2$$

[2]Different from receive characteristics, i.e., radar SINR and Cramér-Rao bound (CRB), the transmit beampattern is considered from the perspective of transmit characteristic. Designing transmit beampattern can also bring better sensing performance [9].

$$+ \sigma_I^2 \|\mathbf{E}^H \mathbf{G} \mathbf{E}\|_F^2 \le P_1, \quad (8c)$$
$$R \ge r, \quad (8d)$$
$$|e_m|^2 \le p_{max}, \quad 1 \le m \le M, \quad (8e)$$

where P_0 is the maximum transmit power at the BS, P_1 is the maximum transmit power at the active IRS, and r is the required communication rate of the user. Problem (8) is challenging to solve due the nonconvex objective function (8a), nonconvex constraint (8d), two nonconvex quartic terms of $\mathbf{E}$ in constraint (8c), and the coupling of variables.

III. Algorithm Design

In this section, to address the issue of variable coupling, we propose an alternating optimization (AO) algorithm to solve Problem (8).

A. BS Beamforming Optimization

In this subsection, given reflection coefficient matrix $\mathbf{E}$, the optimization subproblem of Problem (8) corresponding to beamforming vector $\mathbf{w}$ is formulated as follows

$$\max_{\mathbf{w}} \ \mathbf{a}^H(\theta)\mathbf{E}\mathbf{H}_{\mathrm{BI}}\mathbf{w}\mathbf{w}^H\mathbf{H}_{\mathrm{BI}}^H\mathbf{E}^H\mathbf{a}(\theta) \quad (9a)$$
$$\text{s.t. } (8b), (8c), (8d). \quad (9b)$$

The nonconvex objective function (9a) and constraint (8d) in Problem (9) make the problem hard to address. In the following, we resort to the majorization-minization (MM) method in [11].

Let $f(\mathbf{w})$ denote the objective function in (9a). Under the MM framework, a concave minorizer of $f(\mathbf{w})$ is given in the following lemma

Lemma 1: For a fixed point $\mathbf{w}^{(\tau)}$, $f(\mathbf{w})$ is minorized by a concave surrogate function $g(\mathbf{w}|\mathbf{w}^{(\tau)})$ given by

$$g(\mathbf{w}|\mathbf{w}^{(\tau)}) = 2\mathrm{Re}\Big(\mathbf{w}^{(\tau),H}\mathbf{A}\mathbf{w}\Big) - \mathbf{w}^{(\tau),H}\mathbf{A}\mathbf{w}^{(\tau)}, \quad (10)$$

where $\mathbf{A} = \mathbf{H}_{\mathrm{BI}}^H\mathbf{E}^H\mathbf{a}(\theta)\mathbf{a}^H(\theta)\mathbf{E}\mathbf{H}_{\mathrm{BI}}$.

Proof: The proof is similar to the proof in [11, Appendix A] and thus omitted, due to limited space. ■

Similarly, by means of the first order Taylor expansion, constraint (8d) can be transformed

$$2\mathrm{Re}\Big(\mathbf{w}^{(\tau),H}\mathbf{B}\mathbf{w}\Big) - \mathbf{w}^{(\tau),H}\mathbf{B}\mathbf{w}^{(\tau)} \ge \Omega_1, \quad (11)$$

where $\mathbf{B} = (\mathbf{h}_{\mathrm{BU}}^H + \mathbf{h}_{\mathrm{IU}}^H\mathbf{E}\mathbf{H}_{\mathrm{BI}})^H(\mathbf{h}_{\mathrm{BU}}^H + \mathbf{h}_{\mathrm{IU}}^H\mathbf{E}\mathbf{H}_{\mathrm{BI}})$ and $\Omega_1 = (2^r - 1)(\sigma_I^2\|\mathbf{h}_{\mathrm{IU}}^H\mathbf{E}\|^2 + \sigma_c^2)$.

Finally, by substituting the objective function (9a) with (10) and the communication rate constraint (8d) with (11), Problem (9) can be recast as

$$\max_{\mathbf{w}} \ 2\mathrm{Re}\Big(\mathbf{w}^{(\tau),H}\mathbf{A}\mathbf{w}\Big) \quad (12a)$$
$$\text{s.t. } 2\,\mathrm{Re}\Big(\mathbf{w}^{(\tau),H}\mathbf{B}\mathbf{w}\Big) - \mathbf{w}^{(\tau),H}\mathbf{B}\mathbf{w}^{(\tau)} \ge \Omega_1, \quad (12b)$$
$$(8b), (8c). \quad (12c)$$

Problem (12) is a second-order cone programming (SOCP) problem which can be solved using CVX directly. Hence, we propose Algorithm 1 to obtain a suboptimal solution to Problem (9).

B. Reflection Coefficients Optimization

In this subsection, given $\mathbf{w}$, the subproblem of Problem (8) corresponding to $\mathbf{E}$ is formulated as follows

Algorithm 1 MM Algorithm for Solving Problem (9)

1: Initialize the tolerance ϵ_1, the beamforming vector $\mathbf{w}^{(0)}$ and the maximum iteration number τ_{max}. Set iteration index $\tau = 0$. Calculate the objective function (9a) $f(\mathbf{w}^{(0)})$.
2: **repeat**
3: Obtain $\mathbf{w}^{(\tau+1)}$ by solving the Problem (12).
4: Set $\tau = \tau + 1$.
5: **until** $|\frac{f(\mathbf{w}^{(\tau+1)}) - f(\mathbf{w}^{(\tau)})}{f(\mathbf{w}^{(\tau)})}| \le \epsilon_1$ or $\tau > \tau_{max}$.

$$\max_{\mathbf{E}} \ (8a) \quad (13a)$$
$$\text{s.t. } (8c), (8d), (8e). \quad (13b)$$

Denoting by $\mathbf{e} = [e_1, e_2, \ldots, e_M]^H \in \mathbb{C}^{M\times 1}$ the vector containing the diagonal elements of $\mathbf{E}$, by $\widetilde{\mathbf{e}} = [\mathbf{e}^H, 1]^H \in \mathbb{C}^{(M+1)\times 1}$ the vector containing $\mathbf{e}$ and 1, and by $\widetilde{\mathbf{H}} = [\mathbf{H}_{\mathrm{BI}}^H\mathrm{diag}(\mathbf{h}_{\mathrm{IU}}^H)^H, \mathbf{h}_{\mathrm{BU}}]^H$ the equivalent channel between the BS and the user, the transmission rate constraint (8d) can be rewritten as follows

$$|\widetilde{\mathbf{e}}^H\widetilde{\mathbf{H}}\mathbf{w}|^2 \ge \Omega_2(\sigma_I^2\mathbf{e}^H\mathrm{diag}(\mathbf{h}_{\mathrm{IU}}^H)\mathrm{diag}(\mathbf{h}_{\mathrm{IU}}^H)^H\mathbf{e} + \sigma_c^2), \quad (14)$$

where $\Omega_2 = 2^r - 1$.

Let $\widetilde{\mathbf{E}} = \widetilde{\mathbf{e}}\widetilde{\mathbf{e}}^H$, (14) can be further transformed as

$$\Omega_2(\sigma_I^2\mathrm{Tr}(\mathrm{diag}(\mathbf{h}_{\mathrm{IU}}^H)\mathrm{diag}(\mathbf{h}_{\mathrm{IU}}^H)^H[\widetilde{\mathbf{E}}]_{1:M,1:M}) + \sigma_c^2) - \mathrm{Tr}(\widetilde{\mathbf{H}}\mathbf{w}\mathbf{w}^H\widetilde{\mathbf{H}}^H\widetilde{\mathbf{E}}) \le 0. \quad (15)$$

Next, to address the nonconvex constraint (8c), we first exploit the following equation:

$$\mathrm{vec}(\mathbf{E}^H\mathbf{C}\mathbf{E}) = (\mathbf{E}^T \otimes \mathbf{E}^H)\,\mathrm{vec}(\mathbf{C}) = \mathrm{diag}(\mathrm{vec}(\mathbf{C}))\bar{\mathbf{e}}, \quad (16)$$

where $\mathbf{C}$ is an arbitrary matrix, and $\bar{\mathbf{e}}$ is the vector containing diagonal elements of matrix $\mathbf{E}^T \otimes \mathbf{E}^H$, i.e., $\bar{\mathbf{e}} = \mathrm{vec}([\widetilde{\mathbf{E}}]_{1:M,1:M})$. Based on (16) and the property $\mathrm{Tr}(\mathbf{ABCD}) = (\mathrm{vec}(\mathbf{D}^T))^T(\mathbf{C}^T \otimes \mathbf{A})\,\mathrm{vec}(\mathbf{B})$, constraint (8c) can be transformed into

$$\Big[\mathrm{vec}^T(\mathbf{I}_M)\Big(\mathrm{diag}(\mathrm{vec}(\mathbf{D})) + (\sigma_I^2 + \sigma_p^2)\mathrm{diag}(\mathrm{vec}(\mathbf{I}_M))\Big)\Big]$$
$$\mathrm{vec}^*([\widetilde{\mathbf{E}}]_{1:M,1:M}) + \mathrm{vec}^H([\widetilde{\mathbf{E}}]_{1:M,1:M})\Big[\mathrm{diag}(\mathrm{vec}(\mathbf{G}))^H$$
$$(\mathbf{D}^* \otimes \mathbf{I}_M)\mathrm{diag}(\mathrm{vec}(\mathbf{G})) + \sigma_I^2\mathrm{diag}(\mathrm{vec}(\mathbf{G}))^H\mathrm{diag}(\mathrm{vec}(\mathbf{G}))\Big]$$
$$\mathrm{vec}([\widetilde{\mathbf{E}}]_{1:M,1:M}) - P_1 \le 0, \quad (17)$$

where $\mathbf{D} = \mathbf{H}_{\mathrm{BI}}\mathbf{w}\mathbf{w}^H\mathbf{H}_{\mathrm{BI}}^H$, two quartic terms are transformed into a quadratic term of $\mathrm{vec}([\widetilde{\mathbf{E}}]_{1:M,1:M})$, and the linear term of $\mathrm{vec}([\widetilde{\mathbf{E}}]_{1:M,1:M})$ is derived from the first two quadratic terms in constraint (8c).

Moreover, using some trace operations, the objective function (13a) can be rewritten as follows

$$\mathrm{Tr}\Big(\mathbf{F}[\widetilde{\mathbf{E}}]_{1:M,1:M}\Big) + \sigma_I^2\,\mathrm{Tr}\Big(\mathbf{J}[\widetilde{\mathbf{E}}]_{1:M,1:M}\Big), \quad (18)$$

where $\mathbf{F} = \mathrm{diag}(\mathbf{a}^H(\theta))\mathbf{H}_{\mathrm{BI}}\mathbf{w}\mathbf{w}^H\mathbf{H}_{\mathrm{BI}}^H\mathrm{diag}(\mathbf{a}(\theta))$ and $\mathbf{J} = \mathrm{diag}(\mathbf{a}^H(\theta))\mathrm{diag}(\mathbf{a}(\theta))$.

Finally, combining (15), (17), and (18), Problem (13) is equivalent to

$$\max_{\widetilde{\mathbf{E}}} \ (18) \quad (19a)$$
$$\text{s.t. } (17), (15), \quad (19b)$$

Algorithm 2 AO Algorithm for Solving Problem (8)

Initialize the tolerance ϵ_2, the reflection coefficient matrix $\mathbf{E}^{(0)}$ of which the diagonal elements are all 1, the maximum ratio transmission beamforming vector $\mathbf{w}^{(0)}$, and the maximum iteration number υ_{max}. Set iteration index $\upsilon = 0$. Let the objective function (8a) denoted by $h(\mathbf{w}, \mathbf{E})$ and calculate $h(\mathbf{w}^{(0)}, \mathbf{E}^{(0)})$.
repeat
    Given $\mathbf{E}^{(\upsilon)}$, calculate $\mathbf{w}^{(\upsilon+1)}$ by Algorithm 1.
    Given $\mathbf{w}^{(\upsilon+1)}$, calculate $\mathbf{E}^{(\upsilon+1)}$ by solving Problem (19) without rank one constraint. Then, construct rank one solution by Gaussian randomization method.
    Set $\upsilon = \upsilon + 1$ and calculate the objective function $h(\mathbf{w}^{(\upsilon+1)}, \mathbf{E}^{(\upsilon+1)})$.
until $\left|\frac{h(\mathbf{w}^{(\upsilon+1)},\mathbf{E}^{(\upsilon+1)})-h(\mathbf{w}^{(\upsilon)},\mathbf{E}^{(\upsilon)})}{h(\mathbf{w}^{(\upsilon)},\mathbf{E}^{(\upsilon)})}\right| \le \epsilon_2$ or $\upsilon > \upsilon_{max}$.

$$0 < [\mathrm{diag}(\widetilde{\mathbf{E}})]_m \le p_{max}, \quad 1 \le m \le M, \tag{19c}$$
$$[\mathrm{diag}(\widetilde{\mathbf{E}})]_{M+1} = 1, \tag{19d}$$
$$\widetilde{\mathbf{E}} \succeq \mathbf{0}, \mathrm{rank}(\widetilde{\mathbf{E}}) = 1. \tag{19e}$$

Here, by dropping the rank one constraint, Problem (19) is a standard semidefinite programming (SDP) which can be solved using CVX. Then, a suboptimal rank-one solution can be obtained by using the Gaussian randomization method [12]. Let $\widetilde{\mathbf{E}}_1$ be the rank-one relaxed solution to Problem (19), and the eigenvalue decomposition of $\widetilde{\mathbf{E}}_1$ is represented by $\widetilde{\mathbf{E}}_1 = \mathbf{U}\mathbf{\Sigma}\mathbf{U}^H$ where the columns of $\mathbf{U}$ are eigenvectors of $\widetilde{\mathbf{E}}_1$ and $\mathbf{\Sigma}$ is a diagonal matrix including the eigenvalues of $\widetilde{\mathbf{E}}_1$. More specifically, 5000 random candidate vectors are generated, i.e., $\widetilde{\mathbf{e}}_i = \frac{\mathbf{U}\mathbf{\Sigma}^{\frac{1}{2}}\mathbf{v}_i}{[\mathbf{U}\mathbf{\Sigma}^{\frac{1}{2}}\mathbf{v}_i]_{M+1}}, i = 1, \ldots, 5000$ where $\mathbf{v}_i \sim \mathcal{CN}(0, \mathbf{I}_{M+1})$. Then, the $\widetilde{\mathbf{E}}_i = [\mathrm{diag}(\widetilde{\mathbf{e}}_i^*)]_{1:M,1:M}$ that satisfies all the constraints in Problem (13) and maximizes the objective function (13a) is selected as the optimal solution. Note that rank-one solution obtained by Gaussian randomization technique may decrease the objective function (8a). So, in order to guarantee the convergence of the AO algorithm, a large number of Gaussian randomization should be implemented to ensure that the objective function (8a) is non-decreasing at every alternating iteration [1], [6].

In the end, the overall AO method is summarized in Algorithm 2.

C. Convergence and Complexity Analysis

1) Convergence: First, in Algorithm 1, given $\mathbf{E}^{(\upsilon)}$, we have

$$f(\mathbf{w}^{(\tau)}|\mathbf{E}^{(\upsilon)}) = g(\mathbf{w}^{(\tau)}|\mathbf{w}^{(\tau)}, \mathbf{E}^{(\upsilon)}) \le g(\mathbf{w}^{(\tau+1)}|\mathbf{w}^{(\tau)}, \mathbf{E}^{(\upsilon)}) \le f(\mathbf{w}^{(\tau+1)}|\mathbf{E}^{(\upsilon)}), \tag{20}$$

where the first equality follows from the conditions of the MM method, i.e., (A1) in [11], and the second inequality follows from the condition (A2) in [11]. Moreover, with the bounded feasible set, the non-decreasing objective function (9a) has an finite upper bound. Hence, Algorithm 1 is guaranteed to converge. Second, the sequence of objective function generated by Algorithm 2, i.e., $h(\mathbf{w}^{(\upsilon)}, \mathbf{E}^{(\upsilon)})$, is non-decreasing. Similarly, due to the bounded feasible set, the objective function (8a) has an finite upper bound. So, the convergence of Algorithm 2 is also guaranteed.

2) Complexity: The complexity of Algorithm 1 is from solving the SOCP problem (12). So, the main computational complexity of Algorithm 1 per iteration is $\mathcal{O}(N_T 3^{3.5} + N_T^3 3^{2.5})$ where there are three SOC constraints with dimension N_T [11]. Then, the main complexity of solving the SDP problem (19) is $\mathcal{O}(\max\{M+1, 3\}^4 (M+1)^{\frac{1}{2}} \log(\frac{1}{\zeta}))$, where ζ is the given solution accuracy [12]. Hence, the main complexity of Algorithm 2 per iteration is $\mathcal{O}(N_T 3^{3.5} + N_T^3 3^{2.5} + \max\{M+1, 3\}^4 (M+1)^{\frac{1}{2}} \log(\frac{1}{\zeta}))$. In addition, the complexity of Algorithm 2 is much lower than that of [4, Algorithm 1].

IV. Numerical Results

In this section, we provide numerical results to evaluate the performance of the active IRS-aided ISAC systems. The DFRC BS and the active IRS are equipped with $N_T = N_R = 8$ antennas and $M = 32$ reflecting elements, respectively. The locations of the BS, active IRS and the user in rectangular coordinate are (0m, 0m), (50m, 10m) and (80m, 0m), respectively. We assume that the channel $\mathbf{H}_{\mathrm{BI}}$ only contains the line-of-sight (LoS) link modeled as the product of the transmit and receive steering vectors, and channels $\mathbf{h}_{\mathrm{IU}}$ and $\mathbf{h}_{\mathrm{BU}}$ follow Rician distributions with Rician factors of 0.5. Then, the large-scale path loss coefficient is $-30 - 10\alpha \log_{10}(d)$ dB where d is the distance in meters, and the path loss exponents α for the BS-IRS link, the BS-user link, and the IRS-user link are set to 2.5, 3.5, and 2.5, respectively. The angle of the desired point target to be sensed is $\theta = 0°$ relative to the IRS, and the complex amplitude[3] of its echo signal is set as $\beta = 1$. Unless specified otherwise, the maximum BS transmit power is $P_0 = 30$ dBm, the maximum active IRS transmit power is $P_1 = 20$ dBm, and the noise power is $\sigma_I^2 = \sigma_p^2 = \sigma_c^2 = -80$ dBm. Furthermore, the required communication rate is set as $r = 4$ bps/Hz. Finally, the stopping criteria of Algorithms 1 and 2 are set to $\epsilon_1 = \epsilon_2 = 10^{-5}$.

The proposed scheme in this letter is denoted by "**Act.**". For comparison, we also consider three benchmark schemes.

1) "**Pas.**": In this scenario, the passive IRS is deployed to assist the sensing and communication tasks. So, there isn't IRS power constraint (8c) and the AWGN caused by amplifiers, i.e., $\sigma_I^2 = \sigma_p^2 = 0$. Furthermore, the reflection gain constraint, i.e., $|e_m| = 1, 1 \le m \le M$, must be satisfied.

2) "**Act. SO**": In this scenario, the communication task is not considered and the active IRS is only deployed to assist the sensing task. Thus, this problem is similar to (8), but without communication rate constraint (8d).

3) "**Act. SDR**": In order to compare with the MM method, Problem (9) is solved by SDR and Gaussian randomization methods. The subproblem of E is solved as in Algorithm 2.

Fig. 2 illustrates the beampatterns at the active or the passive IRS obtained by different schemes. When the total transmit power, i.e., $P_0 + P_1$, and the number of reflecting elements are the same, the beampattern at the active IRS has a higher mainlobe than the beampattern at the passive IRS, and there is only a trivial gap in the mainlobe of the active IRS with both communication and sensing compared to the sensing only active IRS system. Then, from the comparison of the three active IRS beampatterns, more reflecting elements can achieve better beampattern due to the increased diversity gain.

Fig. 3 shows the beampattern gain versus required communication rate. When the target rate is greater than or equal to 5

[3] Similar to [4], an ideal complex amplitude without considering the pathloss of the echo signal is used in this letter. Additionally, Swerling 5 model is used in our paper, which has a constant complex amplitude.

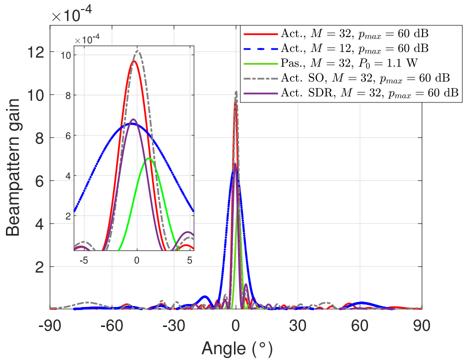

Fig. 2. Beampatterns.

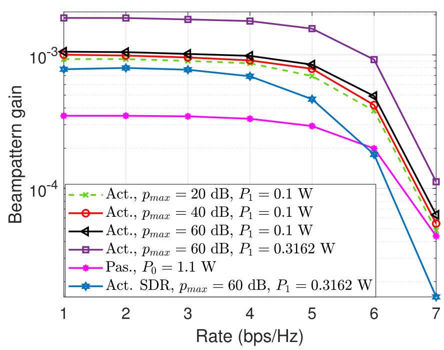

Fig. 3. Beampattern gain versus required communication rate.

bps/Hz, the beampattern gains of all schemes gradually suffer from remarkable loss. Moreover, on the premise of the same total transmit power, the gap of beampattern gains between the active IRS and the passive IRS becomes smaller with the increase of r except the scheme of active IRS based on SDR. This is because more power is consumed by the communication task, and thus, the sensing task is affected severely. Additionally, when the rate is 7 bps/Hz, the scheme of active IRS based on SDR is even worse than the scheme of passive IRS based on MM. This is because Gaussian randomization method cannot find a feasible BS beamforming vector when the rate is too large. Then, when $P_1 = 0.1$ W, there is slight improvement on the beampattern gain at the active IRS by increasing the maximum amplification gain p_{max} from 20 dB to 60 dB. However, increasing P_1 to 0.3162 W leads to a significant beampattern gain improvement. This depicts that the limited IRS transmit power restricts the beampattern gain design.

Fig. 4 plots the beampattern gain versus the number of reflecting elements. It can be seen that the beampattern gains of all schemes can be improved with more reflecting elements. Compared with passive IRS, active IRS can provide acceptable beampattern gain even with a small $M = 12$. This shows that when the total transmit power is the same, active IRS can overcome severe product attenuation and achieve better sensing performance compared to the passive IRS. Same as Figs. 2 and 3, for active IRS, the scheme based on MM is much better than the scheme based on SDR.

V. Conclusion

In this letter, we investigated the DFRC beamforming design for active IRS-aided ISAC systems, where the target is sensed through the BS-IRS-target-IRS-BS link and the user receives

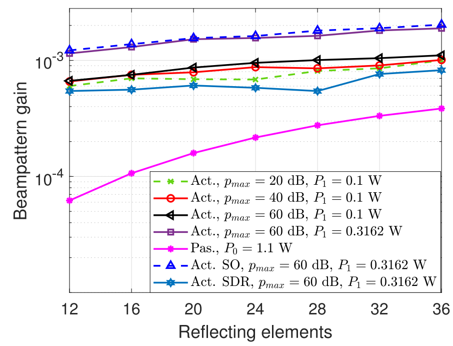

Fig. 4. Beampattern gain versus the number of reflecting elements.

communication signal from both the BS-user and the BS-IRS-user links. An AO algorithm was developed to solve the optimization problem based on the MM, SDR, and Gaussian randomization methods. Numerical results demonstrated that active IRS can significantly improve the beampattern gains even when using less reflecting elements, compared to passive IRS. Compared to amplified and forward (AF) relay-aided ISAC systems, active IRS-aided ISAC systems have simpler hardware architecture, better energy efficiency and more concise beamforming designs. The performance comparison between these two systems will be left as future work. Other future research directions include adjusting the number of active reflecting elements in IRS dynamically, the case of imperfect CSI, multiple communication users, and the analysis of channel training overhead.

References

[1] X. Song, D. Zhao, H. Hua, T. X. Han, X. Yang, and J. Xu, "Joint transmit and reflective beamforming for IRS-assisted integrated sensing and communication," in *Proc. IEEE Wireless Commun. Netw. Conf. (WCNC)*, Austin, TX, USA, 2022, pp. 189–194.

[2] R. Liu, M. Li, H. Luo, Q. Liu, and A. L. Swindlehurst, "Integrated sensing and communication with reconfigurable intelligent surfaces: Opportunities, applications, and future directions," 2022, *arXiv:2206.08518*.

[3] Z. Zhang et al., "Active RIS vs. passive RIS: Which will prevail in 6G?," *IEEE Trans. Commun.*, vol. 71, no. 3, pp. 1707–1725, Mar. 2023.

[4] A. A. Salem, M. H. Ismail, and A. S. Ibrahim, "Active reconfigurable intelligent surface-assisted MISO integrated sensing and communication systems for secure operation," *IEEE Trans. Veh. Technol.*, vol. 72, no. 4, pp. 4919–4931, Apr. 2023.

[5] X. Guan, Q. Wu, and R. Zhang, "Anchor-assisted channel estimation for intelligent reflecting surface aided multiuser communication," *IEEE Trans. Wireless Commun.*, vol. 21, no. 6, pp. 3764–3778, Jun. 2022.

[6] Z.-M. Jiang et al., "Intelligent reflecting surface aided dual-function radar and communication system," *IEEE Syst. J.*, vol. 16, no. 1, pp. 475–486, Mar. 2022.

[7] B. Tang and J. Li, "Spectrally constrained MIMO radar waveform design based on mutual information," *IEEE Trans. Signal Process.*, vol. 67, no. 3, pp. 821–834, Feb. 2019.

[8] J. Li and P. Stoica, "MIMO radar with colocated antennas," *IEEE Signal Process. Mag.*, vol. 24, no. 5, pp. 106–114, Sep. 2007.

[9] P. Stoica, J. Li, and Y. Xie, "On probing signal design for MIMO radar," *IEEE Trans. Signal Process.*, vol. 55, no. 8, pp. 4151–4161, Aug. 2007.

[10] M. Hua, Q. Wu, W. Chen, O. A. Dobre, and A. L. Swindlehurst, "Secure intelligent reflecting surface aided integrated sensing and communication," 2022, *arXiv:2207.09095*.

[11] G. Zhou, C. Pan, H. Ren, K. Wang, and A. Nallanathan, "Intelligent reflecting surface aided multigroup multicast MISO communication systems," *IEEE Trans. Signal Process.*, vol. 68, pp. 3236–3251, Apr. 2020.

[12] Z.-Q. Luo, W.-K. Ma, A. M.-C. So, Y. Ye, and S. Zhang, "Semidefinite relaxation of quadratic optimization problems," *IEEE Signal Process. Mag.*, vol. 27, no. 3, pp. 20–34, May 2010.